

# ЭЛЕКТРОТЕХНОЛОГИИ И ЭЛЕКТРООБОРУДОВАНИЕ / ELECTRICAL TECHNOLOGIES AND EQUIPMENT

УДК 542.467

doi: 10.15507/2658-4123.032.202203.423-436

Original article



## Flow Boiling Heat Transfer of Grooved Copper Foam with Open Gap

D. Zhang<sup>a</sup>✉, L. Sun<sup>a</sup>, J. Mao<sup>a</sup>, Q. Lei<sup>a</sup>, D. Chen<sup>a</sup>, A. P. Levstev<sup>b</sup><sup>a</sup> Jiangsu University of Science and Technology (Zhenjiang, China)<sup>b</sup> National Research Mordovia State University  
(Saransk, Russian Federation)✉ [dhzhang20@126.com](mailto:dhzhang20@126.com)

### Abstract

**Introduction.** Copper foam material has various advantages. It has been proved effective in enhanced boiling heat transfer, but also increases pump power consumption. Grooved copper foam is a solution to achieve good balance between boiling heat transfer characteristics and pump power consumption.

**Material and Methods.** Grooveless and grooved copper foam in open space was studied. Copper foam specifications comprised the combination of porosities of 70, 80 and 90%, and pore densities of 90 and 110 PPI. The grooved copper foams have two specifications: 11 and 17 grooves. The corresponding rib widths are 2 and 1 mm, with groove depth 2.9 mm and width 0.6 mm. The flow boiling experimental system of copper foam sample includes four parts: a heating water reservoir, pump, a test section, and a data acquisition system. In the test section, liquid water turns into vapor and carries the heat away from a copper block surface, and then vapor condenses into liquid water in the terminal reservoir.

**Results.** Grooved copper foam samples presented significantly higher efficiency than grooveless ones. Grooved copper foams can increase the critical heat flux and heat transfer coefficient, compared with grooveless ones. Seventeen-grooved samples showed more excellent performance than 11-grooved ones. Visual observation disclosed that the stratified flow pattern dominated in moderate and high heat flux for grooved copper foam with open space. Covering vapor mass was more effective to be formed above 17-grooved samples, compared with 11-grooved ones. It indicated more vigorous boiling behavior occurs in 17-grooved sample.

**Discussion and Conclusion.** The number of grooves has a significant impact on boiling heat transfer. Grooved copper foam samples present a significantly higher critical heat flux and heat transfer coefficient. Structural parameters such as porosity and pore density, play a relatively secondly role in heat transfer argumentation. Visual observation shows there exists a cyclic alternation of flow patterns: bubbly flow, annular flow and mass vapor

© Zhang D., Sun L., Mao J., Lei Q., Chen D., Levstev A. P., 2022

Контент доступен по лицензии Creative Commons Attribution 4.0 License.  
This work is licensed under a Creative Commons Attribution 4.0 License.

formation for grooved samples. Forming vapor mass is more effective to be formed in 17-grooved samples, compared to 11-grooved ones. It indicates more vigorous boiling behavior occurs in 17-grooved samples.

**Keywords:** copper foam, boiling heat transfer, bubbling dynamics, flow pattern, heat transfer enhancement

**Funding:** We gratefully acknowledge the financial support of Sino-Russian Joint Laboratory Project.

**Conflict of interest:** The authors declare that they have no known competing financial interests or personal relationships that could have appeared to influence the work reported in this paper.

**For citation:** Zhang D., Sun L., Mao J., et al. Flow Boiling Heat Transfer of Grooved Copper Foam with Open Gap. *Engineering Technologies and Systems*. 2022;32(3):423–436. doi: <https://doi.org/10.15507/2658-4123.032.202203.423-436>

Научная статья

## Теплопередача кипящего потока в слое рифленого медного пеноматериала с открытыми порами

Д. Чжань<sup>1</sup>✉, Л. Сунь<sup>1</sup>, Ц. Мао<sup>1</sup>, Ц. Лей<sup>1</sup>, Д. Чжень<sup>1</sup>,  
А. П. Левцев<sup>2</sup>

<sup>1</sup> Цзянсуский университет науки и технологии  
(г. Чжэньцзян, Китай)

<sup>2</sup> Национальный исследовательский Мордовский  
государственный университет  
(г. Саранск, Российская Федерация)

✉ [dhzhang20@126.com](mailto:dhzhang20@126.com)

### Аннотация

**Введение.** Медный пеноматериал обладает рядом преимуществ. Доказано, что он улучшает теплопередачу при кипении, но увеличивает энергозатраты насоса. Рифленая медная пена позволит достичь оптимального баланса между характеристиками теплопередачи при кипении и потребляемой мощностью насоса.

**Материалы и методы.** Исследован обычный медный пеноматериал и рифленый. Технические характеристики медного пеноматериала представлены комбинациями с пористостью 70, 80 и 90 % и плотностью пор 90 и 110 PPI. Рифленый медный материал имеет 11 и 17 канавок. Соответственно, ширина ребер составляет 2 и 1 мм при глубине канавок 2,9 мм и ширине 0,6 мм. Экспериментальная установка проточного кипения воды в слое пеноматериала состоит из четырех частей: резервуар для нагреваемой воды, насос, испытательная секция и система сбора данных. В испытательной секции жидкая вода превращается в пар и отводит тепло от поверхности медного блока, а затем пар конденсируется в жидкую воду в конечном резервуаре.

**Результаты исследования.** Образцы рифленого медного пеноматериала показали более высокую эффективность, чем образцы обычного. Медный рифленый пеноматериал может повысить критический тепловой поток и коэффициент теплопередачи по сравнению с обычным пеноматериалом. Образцы с 17 канавками показали более высокие показатели, чем образцы с 11 канавками. Визуальное наблюдение показало, что при умеренном и высоком тепловом потоке для рифленого медного пеноматериала с открытыми порами преобладает сложная структура потока. Масса пузырьков пара лучше формировалась над образцами с 17 канавками по сравнению с образцами с 11 канавками. Следовательно, в образце с 17 канавками более интенсивное кипение.

*Обсуждение и заключение.* Количество канавок оказывает существенное влияние на теплопередачу при кипении. Образцы медного рифленого пеноматериала обладают более высоким коэффициентом теплопередачи и критическим тепловым потоком. Структурные параметры, такие как пористость и плотность, оказывают второстепенное влияние на теплопередачу. Визуальное наблюдение показывает, что осуществляется циклическое чередование режимов потока: пузырьковый поток, кольцевой поток и массовое образование пара для образцов с канавками. Большая масса пара образуется на образцах с 17 канавками из-за более интенсивного кипения.

**Ключевые слова:** медный пеноматериал, теплопередача при кипении, динамика барботажа, схема течения, улучшение теплопередачи

**Финансирование:** мы благодарим за финансовую поддержку китайско-российский совместный лабораторный проект.

**Конфликт интересов:** авторы заявляют, что у них нет известных конкурирующих финансовых интересов или личных отношений, которые могли бы повлиять на работу, представленную в данной статье.

**Для цитирования:** Теплопередача кипящего потока в слое рифленого медного пеноматериала с открытыми порами / Д. Чжань [и др.] // Инженерные технологии и системы. 2022. Т. 32, № 3. С. 423–436. doi: <https://doi.org/10.15507/2658-4123.032.202203.423-436>

## Introduction

Now electronic devices are presenting great challenges for the thermal design. The heat flux for electronic chips has out-reached  $200 \text{ W/cm}^2$  in the future. Copper foam has attracted much attention in recent years due to several advantages: very large surface to volume ratio, high thermal conductivity, and high interfacial heat transfer coefficient [1; 2]. It has been proved an effective material for enhanced convective heat transfer. Phase-change heat transfer is a kind of heat dissipation method suitable for high-power electronic equipment. It takes away the heat of electronic equipment through the boiling heat transfer process of liquid working fluid, showing good heat dissipation potential. Copper foam material can further enhance boiling heat transfer, which has been confirmed in some studies, but also brings about additional flow resistance loss, resulting in an increase in pump power consumption [3; 4]. Grooved copper foam is a solution to achieve good balance between boiling heat transfer characteristics and pump power consumption.

## Literature Review

Y. Yang, X. Ji, J. Xu et al. investigated thicknesses effect on pool boiling heat transfer using water as working fluid [5; 6].

Compared with the smooth surface, copper foam could reduce the wall superheat at the ONB point, and present 2–3 times in heat transfer coefficient (HTC) than the smooth surface. They demonstrated that there existed optimum pore density and thickness (60 PPI and 4 mm). A. Kouidri studied boiling heat transfer and flow resistance of organic working fluids in metalfoam-filled tubes [7]. Copper foam and nickel foam alloy (porosity is 20%) were applied. In the flow range tested, copper foam could improve the heat transfer coefficient by 1.3 ~ 3.0 times, but it also increases the pressure drop by 42%. The nickel-alloy foam could not achieve favorable enhancement. The authors proposed a novel bi-porous mini channel heat sink sintered with copper woven tape, composed of two kinds of pore structures: cavities formed by copper strands and crevices formed by copper wires [8]. Experimental results showed that bubble nucleation sites were mainly generated from the cavities between copper strands. Bi-porous mini channel presented 1.37 times in HTC higher than that of the traditional channel. J. Shi et al. explored the wettability effect of metal foam on the pool boiling process [9; 10]. Results showed that

the super-hydrophilic sample achieves better boiling heat transfer performance in medium- or high-heat flux region ( $q \geq 20 \text{ W/cm}^2$ ), while super-hydrophobic copper foam surface shows a better performance in low heat flux region. L. Manetti et al. studied the pool boiling heat transfer enhancement of copper foams with different thicknesses (1, 2, 3 mm), using HFE-7100 as working fluid [11]. The HTC of copper foam was significantly improved. When the heat flux is higher than  $20 \text{ W/cm}^2$ , the copper foam with 1 mm thickness showed the best augmenting effect, 145% higher than that of the copper plate surface. Z. G. Xu and C. Y. Zhao studied the effect of thickness of deionized water on boiling heat transfer performance of V-groove horizontal copper foam pool [12]. V-shaped grooves use capillary action and separate vapor-liquid flow path to reduce the flow resistance of escaping vapor bubbles by supplying liquid, and the existence of enough groove structures increases the critical heat flux.

From the current progress, researches on boiling heat transfer enhancement of copper foam were mainly concentrated in the field of pool boiling, and less studies on flow boiling. In the liquid cooling application, introduction of copper foam may greatly increase the flow resistance compared with the empty channel, resulting in an increase in pump power

consumption. The groove structure of copper foam can mitigate the contradiction between these two [13; 14]. On one hand, processed grooves can reduce the flow resistance; on the other hand, it can also help the smooth separation of bubble from liquid and improve the critical heat flux (CHF).

The main objective of this paper is to investigate the effects of grooves number and structural parameters on flow boiling heat transfer for copper foam samples. The experiments were carried out, with deionized water as working fluid. The mechanism of enhanced heat transfer of copper foam was analyzed by visualization.

## Materials and Methods

### Materials

In order to understand the effect of copper foam parameters on heat transfer performance, three groups of porosity samples were studied, which were 70, 80 and 90%, respectively. Each group contains two kinds of pore densities: 90 and 110 PPI. Figure 1 shows copper foam samples without groove (a) and with groove (b). The size of copper foam sample is 28 mm (length)  $\times$  28 mm (width)  $\times$  2 mm (thickness). The grooved copper foams have two specifications: 11 and 17 grooves. The groove is processed by wire cutting method. The corresponding rib widths are 2 and 1 mm, with groove depth 2.9 mm and width 0.6 mm, shown in Figure 2.



a)



b)

Fig. 1. Schematic diagram of channel distribution of copper foam samples: a) grooveless sample; b) grooved sample

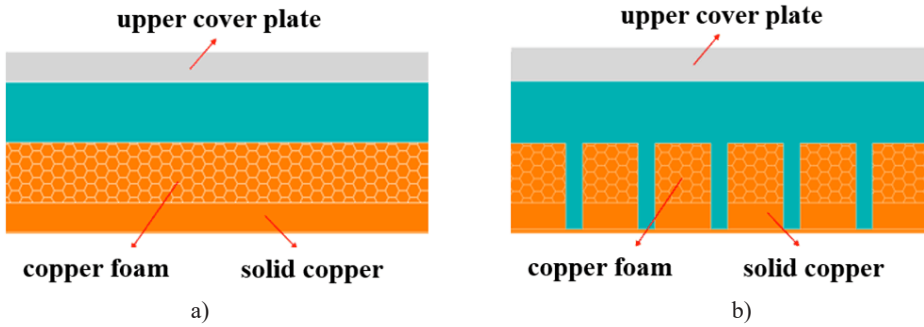


Fig. 2. Cross section diagram of grooveless and grooved copper foam samples

*Experimental system*

The flow boiling experimental system of copper foam sample is shown in Figure 2, including four parts: heating water tank, pump, test section, and data acquisition system. The deionized and degassed water is heated to the experimental setting temperature. It is driven, by a micro gear pump, into the test section. Flow boiling process occurs in the copper foam sample. In the test section, liquid water is transformed into vapor and removes heat from the copper block surface. Subsequently, the vapor is condensed into liquid water in the terminal reservoir. The heating copper module includes a copper block and six heating electric rods, regulated by a DC power supply. The pressure difference between the inlet and outlet of the heat sink is monitored by a differential pressure sensor.

The inlet and outlet fluid temperatures are measured by two PT100 thermocouples. Five T-type thermocouples are used in measuring wall temperature distribution. The measurement data is converted by the NI acquisition card and entered into the computer for real-time display.

Copper foam heat sink is the core part of the experimental system. As shown in Figure 3, the heat sink is composed of upper cover plate, enclosure structure, heated copper block and glass fiber base. Such a design could ensure most of the input heat transferred to deionized water. The upper cover plate is made of PC plate and the enclosure structure is made of PEEK material. The copper foam sample is welded on the top of the heating copper block. The O-type sealing rubber was adopted to ensure no leakage.

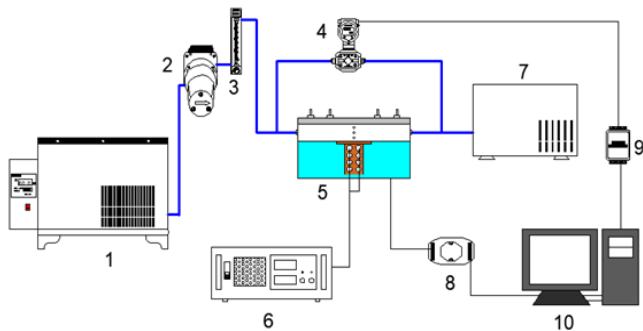


Fig. 3. System diagram: 1 – thermostatic water tank; 2 – micro gear pump; 3 – flowmeter; 4 – differential pressure sensor; 5 – heat sink; 6 – DC power supply; 7 – water reservoir; 8 – NI acquisition card; 9 – temperature converter; 10 – computer

*Data processing and error analysis*  
 Effective heat flux:

$$q_{eff} = q_{total} - q_{loss}, \quad (1)$$

where  $q_{total}$  is the total input heating power;  $q_{loss}$  is the heat loss between heat sink and environment. Boiling heat transfer coefficient is as follows:

$$h = \frac{q_{eff}}{T_w - T_{sat}}, \quad (2)$$

where  $T_w$  is the average surface wall temperature, K;  $T_{sat}$  is the saturation temperature of the working fluid, K;  $T_w$  is extrapolated from the temperature of the uppermost thermocouple point, assuming one-dimensional heat conduction [15]. The saturated pressure is derived by the linear interpolation method in terms of inlet and outlet pressure at each inputting heat flux. The corresponding saturation temperature  $T_{sat}$  is then figured out.

Mass flux:

$$G = \frac{\rho_l q_v}{A_{ch}}, \quad (3)$$

where  $G$  is the mass flux, kg/m<sup>2</sup>·s;  $q_v$  is volume flow, L/h;  $A_{ch}$  is the cross-sectional area of the sample, m<sup>2</sup>.

According to previous researches, it was found that the heat loss of the heat sink was related to the temperature difference between copper block and environment. It is found that there is a linear relationship between the two. Extrapolation method from single-phase measurement is to estimate the heat loss of two-phase process. The linear function was regressed in Figure 4 in the mass flux of 18.6 kg/m<sup>2</sup>·s.

The uncertainties of flow rate, pressure of inlet and outlet, input heat power are  $\pm 4$ ,  $\pm 0.25$  and  $\pm 0.5\%$ , respectively. The fluid temperatures of inlet and outlet are measured by two thermal resistance sensors (PT100) with uncertainties of  $\pm 0.3$  K. Three thermocouples, used in copper surface temperature measurement, had an uncertainty of  $\pm 0.5$  K after calibrated.

### Results

In the experiment, deionized and degassed water was used as the working fluid, the inlet temperature was 60 °C, and the mass fluxes were 9.3, 18.5 and 27.8 kg/(m<sup>2</sup>·s). The study investigated the boiling heat transfer performance of grooveless and grooved copper foam samples. Structural parameters effect, porosity and pore density, were also explored. In the test section, there exists an open gap with a height of 2 mm above the copper foam sample.

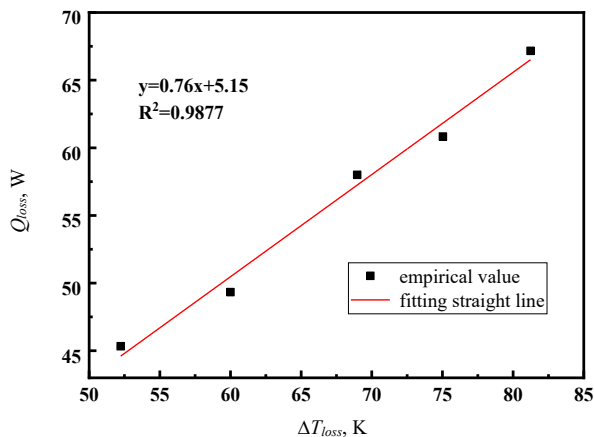


Fig. 4. Fitting line of heat loss and temperature difference

*Effect of groove number on heat transfer performance*

The groove number effects on boiling curves are shown in Figure 5a. Copper foam samples with 90% and 90 PPI were selected. Boiling phenomenon in grooved and grooveless copper foam samples are initiated at the superheat of 4–5 K. After initiation, grooved samples present significantly lower wall superheat than grooveless ones. Moreover, grooved samples could achieve 110 W/cm<sup>2</sup> in CHF while grooveless ones only 90 W/cm<sup>2</sup>. When the heat flux is lower than 65 W/cm<sup>2</sup>, two specifications of grooved samples bear the same trends in boiling curves. These two grooved samples begin to differentiate in performance. The 17-grooved sample maintains lower wall superheat degrees than the 11-grooved one. Compared with grooved samples, the boiling curve slope of the grooveless sample is relatively gentle, indicating high operation wall temperature at the same heat flux. It demonstrates that grooved copper foam could greatly enhance the boiling heat transfer performance.

Corresponding HTC curves are displayed in Figure 5b for copper foam samples with 90% and 90 PPI. From Figure 5b, two grooved samples are almost similar in

performance with that of the grooveless sample in the single-phase region. After larger than 10 W/cm<sup>2</sup>, HTC curves of two grooved samples increase more rapidly than the grooveless sample. When the heat flux is larger than 60 W/cm<sup>2</sup>, the HTC curves of 17-grooved samples continue to exhibit an increase trend while that of 11-grooved begins to fall gently. Seventeen-groove copper foam reaches the largest HTC of 100 kW/(m<sup>2</sup>·K) in the heat flux of 123 W/cm<sup>2</sup>, which is three times as large as that of grooveless sample.

For grooved copper foam with open space, the liquid coolant could be sucked into the heating surface from the porous layer and fins. Generated vapor will immediately leave the porous structure and not retard the liquid supply. Gas-liquid separation is achieved in such a grooved structure. Liquid replenishment and vapor discharge are relatively smooth. Owing to this merit, grooved copper foam could significantly promote both HTC and CHF in comparison with grooveless copper foam.

*Effect of structural parameters*

Structural parameters effect, pore density and porosity, are investigated in detail. Figure 6a shows measured boiling curves of 90 PPI samples with different porosity, namely 70, 80 and 90%.

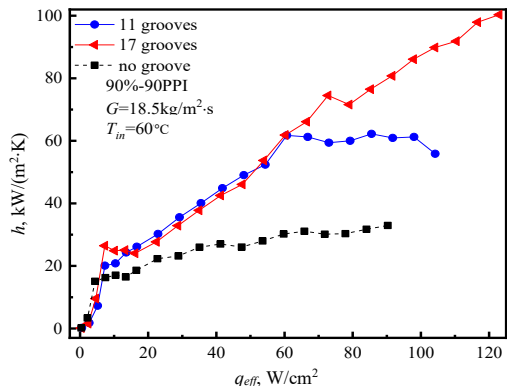
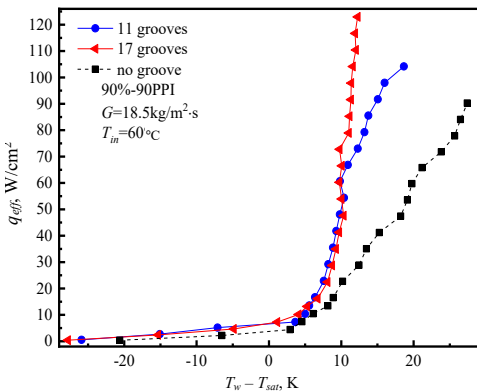


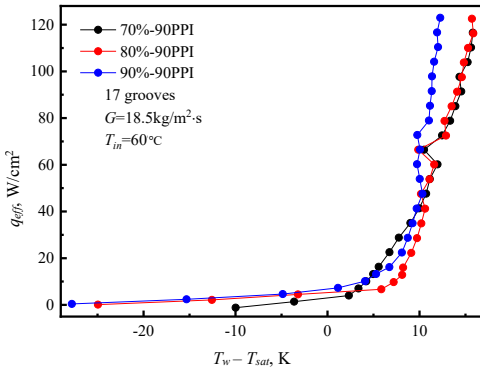
Fig. 5. Boiling curves and HTC curves of grooved and grooveless copper foam samples

Similar boiling curves are observed for three porosities samples. The sample with 70% porosity presents the lowest wall superheat at the heat fluxes of less than 47 W/cm<sup>2</sup>. However, the sample with 90% porosity shows the slightly lowest beyond 47 W/cm<sup>2</sup>. For CHF, three samples could reach 120 W/cm<sup>2</sup> finally.

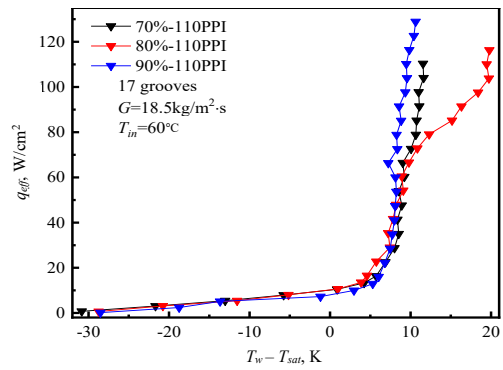
Figure 6b shows the boiling curves of 110 PPI copper foam samples with different porosity. Boiling curves of three samples is similar at  $q \leq 40$  W/cm<sup>2</sup>. When the heat flux is greater than 40 W/cm<sup>2</sup>, the boiling curve of the sample with 90% porosity increases sharply, showing excellent heat transfer performance, and its CHF is 130 W/cm<sup>2</sup>. The copper foam sample with

80% porosity bears highest wall superheat degree and deteriorates beyond 60 W/cm<sup>2</sup>.

Figure 7a illustrates corresponding HTC curves of 90PPI samples. Three curves are almost coincident in the range of 10 ~ 65 W/cm<sup>2</sup>. When the heat flux is greater than 65 W/cm<sup>2</sup>, the HTC of 90% specification increases more rapidly than other two ones. Its HTC can reach 100 kW/(m<sup>2</sup>·K). For 110 PPI samples, corresponding HTC curves of are shown in Figure 7b. Similar to boiling curves, HTC curves of the three samples are almost coincident at  $q \leq 64$  W/cm<sup>2</sup> and then differs. With the increase in heat flux, HTC curves of 70 and 90% continue to rise up, but the HTC of 80% takes on a gradually downward trend.

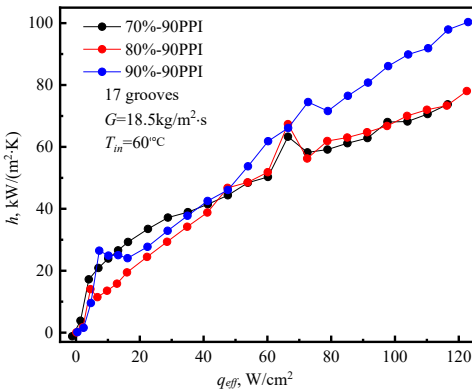


a)

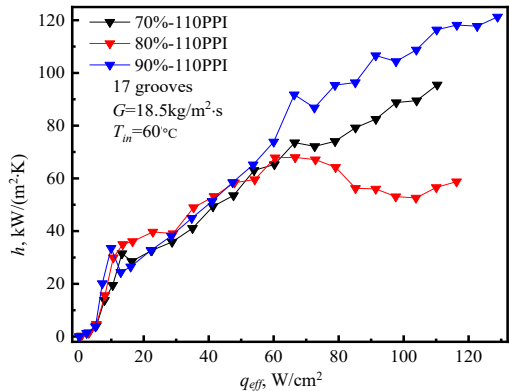


b)

Fig. 6. Boiling curves of grooved copper foam with different porosity



a)



b)

Fig. 7. HTC curves of grooved copper foam with different porosity



The sample of 90% could achieve largest HTC of 121.3 kW/(m<sup>2</sup>·K), twice of 80% sample and far greater than existing literatures.

*Effect of mass flux*

Mass flux influence on flow boiling in grooved copper foam were also studied. Inlet temperature was controlled to 60°C. The 17-groove sample with porosity of 90% and pore densities of 90 PPI was selected.

Figure 8a shows boiling curves at different mass fluxes, namely 9.3, 18.5, 27.8 kg/(m<sup>2</sup>·s). Under low heat fluxes, boiling curves are less affected by the mass flux. It infers that the boiling mechanism is dominated by nucleate boiling. After in medium and high heat flux stage, the mass flux begins to exert an influence on boiling curves. The boiling mechanism switches from nucleate boiling to convection boiling. The wall superheat degree would decrease with the increase in mass flux at the same heat flux. The corresponding heat transfer coefficients are plotted against heat fluxes in Figure 8b. HTC curves show an upward trend under the mass flux of 18.5 and 27.8 kg/(m<sup>2</sup>·s) while HTC curve at  $G = 9.3$  kg/(m<sup>2</sup>·s) shows a trend of increasing first and then decreasing.

*Visualization of grooved copper foam with open gap*

The groove number directly affects the flow pattern after boiling incipience, thus resulting in different heat transfer efficiency. Two samples (90%, 110 PPI) with different groove numbers, 11- and 17-grooved, were selected. The flow patterns of both samples were visualized at different heat flux.

Figure 9 shows the visual images of both of the grooved samples in a low heat flux of 12 W/cm<sup>2</sup>. As shown in Figure 9a, it maintained supercooled liquid state in the upstream section for the 11-grooved sample. Fewer bubbles attached in the wall are observed in the downstream section. Most bubbles could not grow anymore due to low wall superheat. Different from the 11-groove sample, obvious stratification phenomenon is observed in Figure 9b for the 17-groove sample. Many bubbles are generated in the porous wall, and quickly discharge under the action of buoyancy force. The dense bubble layer is formed in the upper cover plate.

As the heat flux is increased to 54 W/cm<sup>2</sup>, both kinds of samples also show great difference. Boiling behaviors of 11-grooved sample are shown in Figure 10a over a period of time. At  $t = 0$  s, the supercooled nuclear boiling occurs in channels. Mainstream liquid contains a large number of small bubbles.

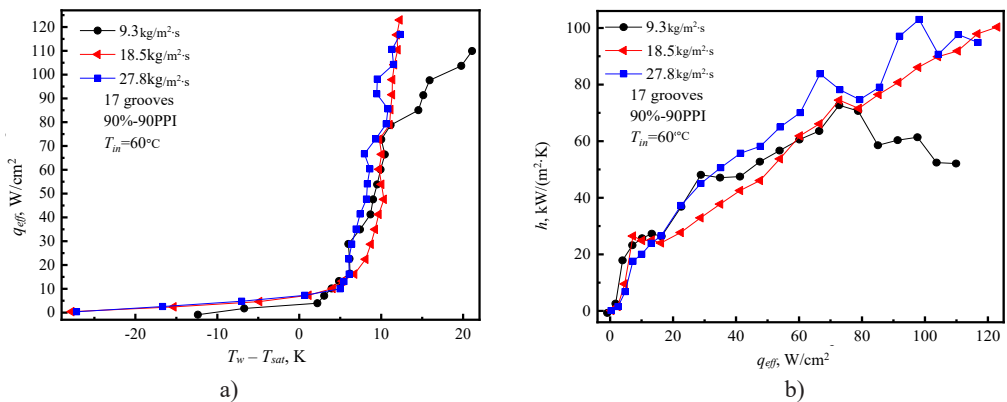


Fig. 8. Boiling curves and HTC curves at different mass fluxes

The flow pattern is dominated by bubbly flow. At  $t = 0.08$  s, annular flow is observed in the downstream section because of coalescence effect (the red coil in the figure).

Boiling behaviors of 17-grooved sample are shown in Figure 10b over a period of time. At  $t = 0$  s, the observed image is analogous to the 11-grooved sample. At  $t = 0.11$  s, a vapor mass is formed in the upstream region. At  $t = 0.97$  s, vapor masses were flushed out of the channel by the mainstream fluid, and its occupied region reduced. There existed a cycle of alternating flow patterns: bubbly flow, annular flow and vapor mass. Such phenomenon presented the periodic characteristics.

When the heat flux continues to increase to  $116.8 \text{ W/cm}^2$ , the 11-groove sample has reached CHF. As shown in Figure 11, at  $t = 0$  s, the vapor mass occupied half of the sample area, and it developed to two thirds area up to  $t = 0.019$  s. The CHF is triggered by large area drought. For the 17-channel sample, the CHF is triggered in a heat flux of  $129 \text{ W/cm}^2$ , which visual image was shown in Figure 12. At  $t = 0$  s, a large vapor mass completely covers the region of one side and results in uneven liquid inflow. After  $0.57$  s, the air mass spreads almost the whole region, only four

channels of one side as liquid inlet. Bubbles are being generated continuously and grew up under the vapor mass. The CHF is also resulted from large area drought.

### Discussion and Conclusion

This work mainly studied boiling heat transfer performance in grooved copper foams. The conclusions are as follows:

1. The groove number has a significant impact on boiling heat transfer. Grooved copper foam samples present significantly higher in enhancement effect than grooveless ones. For grooved copper foam, 17-grooved samples show more superior performance to 11-grooved ones, which could effectively improve CHF and HTC.

2. Compared with groove number effect, porosity and pore density play a relatively minor role in heat transfer argumentation. The copper foam sample with 90% and 110 PPI shows slightly better than other specifications for the grooved samples investigated.

3. Visual observation shows there exists a periodic cycle of alternating flow patterns: bubbly flow, annular flow and vapor mass for grooved samples. Covering vapor mass is more effective to be formed in 17-grooved samples, compared to 11-grooved ones. It indicates more vigorous boiling behavior occurred in the 17-grooved sample.

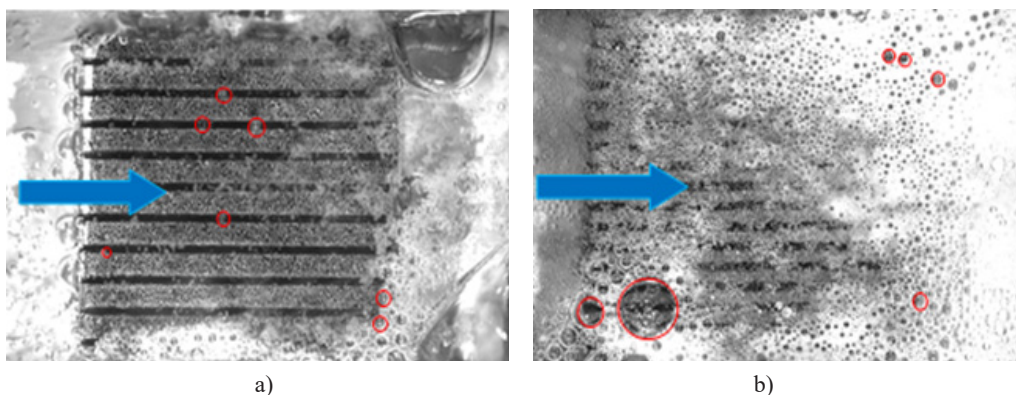
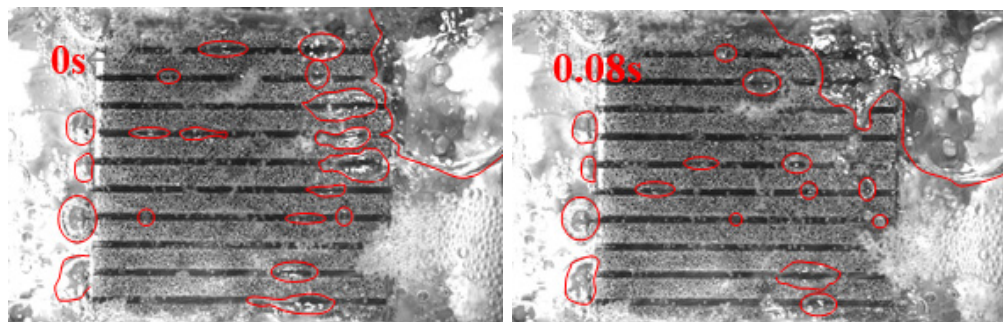
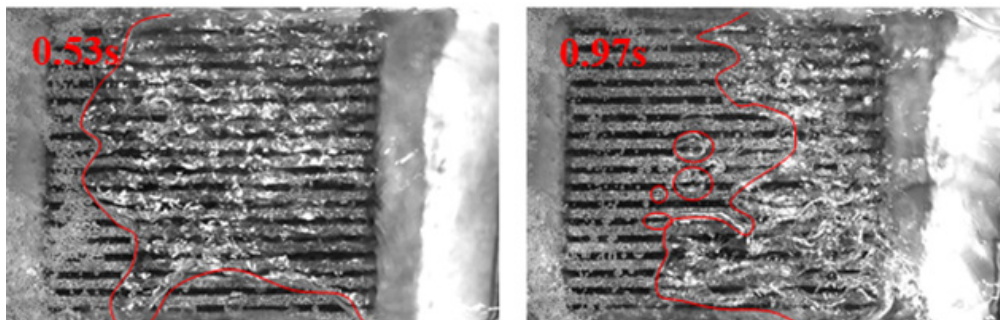
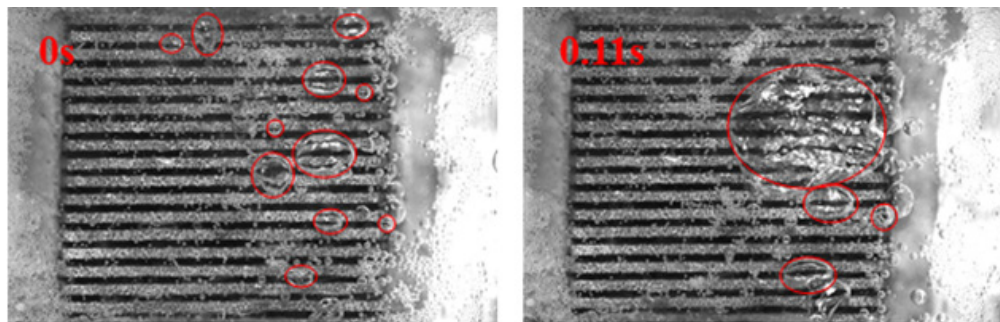


Fig. 9. Visual in the heat flux of  $12 \text{ W/cm}^2$ : a) 11-grooved; b) 17-grooved



a)



b)

Fig. 10. Visual observation in the heat flux of  $54 \text{ W/cm}^2$ : a) 11-grooved sample; b) 17-grooved sample

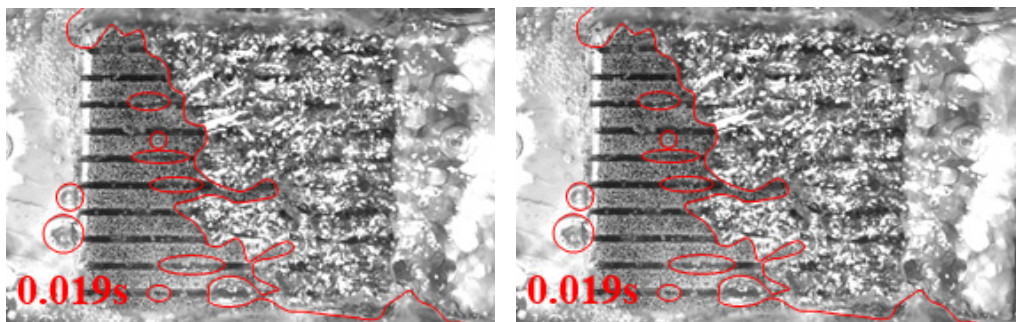


Fig. 11. Visualization at  $q = 116.8 \text{ W/cm}^2$  near CHF for 11-grooved sample

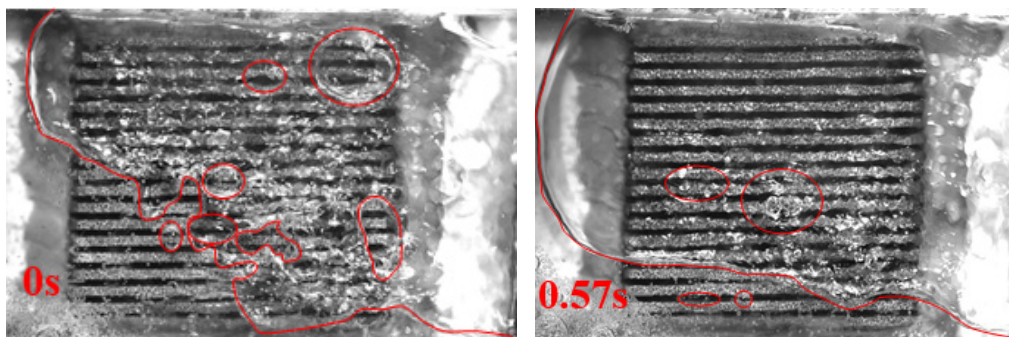


Fig. 12. Visualization at  $q = 129 \text{ W/cm}^2$  near CHF for 17-grooved sample

For the grooved copper foam with open space, the stratified flow pattern dominates in moderate and high heat flux. The CHF mechanism result from large area dry-out induced by continuous covering vapor film.

## REFERENCE

1. Xu Z.G., Zhao C.Y. Experimental Study on Pool Boiling Heat Transfer in Gradient Metal Foams. *International Journal of Heat and Mass Transfer*. 2015;85:824–829. doi: <https://doi.org/10.1016/j.ijheatmasstransfer.2015.02.017>
2. Gao W.H., Xu X., Liang X. Flow Boiling of R134a in an Open-Cell Metal Foam Mini-Channel Evaporator. *International Journal of Heat and Mass Transfer*. 2018;126(A):103–115. doi: <https://doi.org/10.1016/j.ijheatmasstransfer.2018.04.125>
3. Deng D., Zeng L., Sun W. A Review on Flow Boiling Enhancement and Fabrication of Enhanced Microchannels of Microchannel Heat Sinks. *International Journal of Heat and Mass Transfer*. 2021;175. doi: <https://doi.org/10.1016/j.ijheatmasstransfer.2021.121332>
4. Hong S., Dang C., Hihara E. A 3D Inlet Distributor Employing Copper Foam for Liquid Replenishment and Heat Transfer Enhancement in Microchannel Heat Sinks. *International Journal of Heat and Mass Transfer*. 2020;157. doi: <https://doi.org/10.1016/j.ijheatmasstransfer.2020.119934>
5. Yang Y., Ji X., Xu J. Pool Boiling Heat Transfer on Copper Foam Covers with Water as Working Fluid. *International Journal of Thermal Sciences*. 2010;49(7):1227–1237. doi: <https://doi.org/10.1016/j.ijthermalsci.2010.01.013>
6. Xu J., Ji X., Zhang W., Liu G. Pool Boiling Heat Transfer of Ultra-Light Copper Foam with Open Cells. *International Journal of Multiphase Flow*. 2008;34(11):1008–1022. doi: <https://doi.org/10.1016/j.ijmultiphaseflow.2008.05.003>
7. Koudri A., Madani B. Thermal and Hydrodynamic Performance of Flow Boiling Through a Heat Exchanger Filled with Various Metallic Foam Samples. *Chemical Engineering and Processing: Process Intensification*. 2017;121:162–169. doi: <https://doi.org/10.1016/j.cep.2017.08.014>
8. Deng D., Tang Y., Liang D., et al. Flow Boiling Characteristics in Porous Heat Sink with Reentrant Microchannels. *International Journal of Heat and Mass Transfer*. 2020;70. doi: <https://doi.org/10.1016/j.ijheatmasstransfer.2013.10.057>
9. Shi J., Jia X., Feng D., et al. Wettability Effect on Pool Boiling Heat Transfer Using a Multiscale Copper Foam Surface. *International Journal of Heat and Mass Transfer*. 2020;146. doi: <https://doi.org/10.1016/j.ijheatmasstransfer.2019.118726>

10. Shi J., Feng D., Chen Z. Experimental Investigation on Pool Boiling Heat Transfer on Untreated/Super-Hydrophilic Metal Foam under Microgravity. *International Journal of Heat and Mass Transfer*. 2020;151. doi: <https://doi.org/10.1016/j.ijheatmasstransfer.2019.119289>

11. Manetti L.L., Moita A.S.O.H., de Souza R.R., et al. Effect of Copper Foam Thickness on Pool Boiling Heat Transfer of HFE-7100. *International Journal of Heat and Mass Transfer*. 2020;152. doi: <https://doi.org/10.1016/j.ijheatmasstransfer.2020.119547>

12. Xu Z.G., Qu Z.G., Zhao C.Y., et al. Pool Boiling Heat Transfer on Open-Celled Metallic Foam Sintered Surface under Saturation Condition. *International Journal of Heat and Mass Transfer*. 2011;54(17–18):3856–3867. doi: <https://doi.org/10.1016/j.ijheatmasstransfer.2011.04.043>

13. Li H.Y., Leong K.C. Experimental and Numerical Study of Single and Two-Phase Flow and Heat Transfer in Aluminum Foams. *International Journal of Heat and Mass Transfer*. 2011;54(23–24):4904–4912. doi: <https://doi.org/10.1016/j.ijheatmasstransfer.2011.07.002>

14. Tong L., Xiaomin W., Qiang M. Pool Boiling Heat Transfer of R141b on Surfaces Covered Copper Foam with Circular-Shaped Channels. *Experimental Thermal and Fluid Science*. 2019;105:136–143. doi: <https://doi.org/10.1016/j.expthermflusci.2019.03.015>

15. Zhang D.H., Xu H., Chen Y., et al. Boiling Heat Transfer Performance of Parallel Porous Microchannels. *Energies*. 2020;13(11). doi: <https://doi.org/10.3390/en13112970>

*Submitted 12.05.2022; approved after reviewing 08.06.2022; accepted for publication 20.06.2022*  
*Поступила 12.05.2022; одобрена после рецензирования 08.06.2022; принята к публикации 20.06.2022*

*About the authors:*

**Donghui Zhang**, Associate Professor in School of Energy and Power, Jiangsu University of Science and Technology (2 Mengxi Rd, Zhenjiang 212003, China), ORCID: <https://orcid.org/0000-0002-7790-2948>, [dhzhang20@126.com](mailto:dhzhang20@126.com)

**Lili Sun**, Postgraduate Student in School of Energy and Power, Jiangsu University of Science and Technology (2 Mengxi Rd, Zhenjiang 212003, China), [1640880760@qq.com](mailto:1640880760@qq.com)

**Jijin Mao**, Postgraduate Student in School of Energy and Power, Jiangsu University of Science and Technology (2 Mengxi Rd, Zhenjiang 212003, China), [554436558@qq.com](mailto:554436558@qq.com)

**Qinhui Lei**, Postgraduate Student in School of Energy and Power, Jiangsu University of Science and Technology (2 Mengxi Rd, Zhenjiang 212003, China), [1287510323@qq.com](mailto:1287510323@qq.com)

**Daifen Chen**, Leading Researcher of Sino-Russian Joint Laboratory Project, Professor in School of Energy and Power, Jiangsu University of Science and Technology (2 Mengxi Rd, Zhenjiang 212003, China), Ph.D., Professor, ORCID: <https://orcid.org/0000-0002-3070-1989>, [dfchen01@163.com](mailto:dfchen01@163.com)

**Alexey P. Levstev**, Leading Researcher of Sino-Russian Joint Laboratory Project, Head of the Chair of Heat and Power Systems of Institute of Mechanics and Power Engineering, National Research Mordovia State University (68 Bolshevistskaya St., Saransk 430005, Russian Federation), Dr.Sci. (Engr.), Professor, ORCID: <https://orcid.org/0000-0003-2429-6777>, Researcher ID: B-8620-2019, [levstevap@mail.ru](mailto:levstevap@mail.ru)

*Contribution of the authors:*

D. Zhang – analysis of the results, and conclusions.

L. Sun – formulating the research task, conducting experiments.

J. Mao – assistance to conduct experiments.

Q. Lei – cooperation to conduct experiments.

D. Chen – overall design of this research.

A. P. Levstev – overall design of this research.

*All authors have read and approved the final manuscript.*

*Об авторах:*

**Чжань Донгхуй**, доцент Школы энергетики Цзянсуского университета науки и технологий (212003, Китай, г. Чжэньцзян, 2 проезд Менгси), ORCID: <https://orcid.org/0000-0002-7790-2948>, [dhzhang20@126.com](mailto:dhzhang20@126.com)

**Сунь Лили**, аспирант Школы энергетики Цзянсуского университета науки и технологий (212003, Китай, г. Чжэньцзян, 2 проезд Менгси), [1640880760@qq.com](mailto:1640880760@qq.com)

**Мао Цзинцинь**, аспирант Школы энергетики Цзянсуского университета науки и технологий (212003, Китай, г. Чжэньцзян, 2 проезд Менгси), [554436558@qq.com](mailto:554436558@qq.com)

**Лей Циньхуй**, аспирант Школы энергетики Цзянсуского университета науки и технологий (212003, Китай, г. Чжэньцзян, 2 проезд Менгси), [1287510323@qq.com](mailto:1287510323@qq.com)

**Чжень Дайфен**, ведущий научный сотрудник китайско-российского лабораторного проекта, профессор Школы энергетики Цзянсуского университета науки и технологий (212003, Китай, г. Чжэньцзян, 2 проезд Менгси), Ph.D., профессор, ORCID: <https://orcid.org/0000-0002-3070-1989>, [dfchen01@163.com](mailto:dfchen01@163.com)

**Левцев Алексей Павлович**, ведущий научный сотрудник китайско-российского лабораторного проекта, заведующий кафедрой теплоэнергетических систем Института механики и энергетики Национального исследовательского Мордовского государственного университета (430005, Российская Федерация, г. Саранск, ул. Большевикская, д. 68), доктор технических наук, профессор, ORCID: <https://orcid.org/0000-0003-2429-6777>, Researcher ID: [B-8620-2019](https://orcid.org/0000-0003-2429-6777), [levtzevap@mail.ru](mailto:levtzevap@mail.ru)

*Заявленный вклад авторов:*

Д. Чжань – анализ результатов и выводы.

Л. Сунь – формулирование задачи исследования, проведение экспериментов.

Ц. Мао – участие в проведении экспериментов.

Ц. Лей – сотрудничество в проведении экспериментов.

Д. Чжень – общий замысел исследования.

А. П. Левцев – общий замысел исследования.

*Все авторы прочитали и одобрили окончательный вариант рукописи.*